

Biochemical and Biomechanic Integrated Modeling of Bone

Joana de Castro Capacete
joana.castro.capacete@tecnico.ulisboa.pt

Instituto Superior Técnico, Lisboa, Portugal

October 2016

Abstract

Bone is in a constant state of turnover. The remodeling process encompasses resorption, by osteoclasts, followed by formation of new bone by osteoblasts. The work presented here integrates a biochemical model, with a biomechanical remodeling model, in order to evaluate the response of bone to mechanical stimuli, which allows the calculation of the dynamics of cell population, as well as changes in bone mass. The biomechanicochemical processes involved in bone remodeling are described by a system of ODE's, relating the interactions between osteoclasts and osteoblasts, with the mechanical environment, characterized by the strain energy density, obtained using a finite element methodology. The results for a simplified two-dimensional femur bone model showed the influence of the load on the concentration of osteoclasts and osteoblasts and, consequently, in density distribution. The model proved to be a good representation of the bone environment, as the results were in agreement with the biological situation. The expansion of the model to include the effects of myeloma bone disease also lead to results according to expected, with an increase in the number of osteoclasts, followed by a decrease in the number of osteoblasts and a consequent decrease of bone mass, characteristic of this disease.

Keywords: Bone Remodeling, Computational Mechanics, Biomechanics, Myeloma Bone Disease.

1. Introduction

Bone remodeling is a tightly regulated process, in which bone resorption is always followed by bone formation in a site-specific manner, and plays an important role in maintaining the integrity of the skeleton and repairing micro-fractures. Several diseases, such as osteoporosis, Pagets disease and myeloma, influence the remodeling cycle, disturbing its equilibrium. The development of models that integrate the knowledge from bone physiology and that can replicate the biomechanical and biochemical processes involved in bone remodeling is of extreme importance, since these allow the comparison between healthy and pathological states, serving as clinical decision support systems for the implementation of therapeutic regimes and prognostic assessments.

The objective of this work is to develop a model with a simple description of the biochemical interactions between bone cells in bone remodeling, in which the process is triggered by an external mechanical stimulus. This model is further extended to include the myeloma bone disease. One major advantage of this new model is that it has fewer state variables than the current models that consider the influence of the mechanical stimulus [17, 14]. This new approach makes it easier to test the influence of each variable, isolated, which is important for the development of more efficient treatments.

2. Biomedical Concepts

2.1. Bone Remodeling

The process of bone remodeling is usually triggered by an external stimulus, which can take several forms, for example, direct mechanical strain or hormone action on bone cells. Osteoblasts and osteocytes sense these signals and recruit osteoclasts that start removing trenches of bone from the surface of trabecular bone, or forming tunnels into cortical bone. The trenches and tunnels are then filled by osteoblasts, which lay down successive layers of new (unmineralized) bone matrix. The activities of bone cells, more specifically the activities of bone resorption and formation are said to be coupled to one another, ensuring that where bone is removed, new bone will be restored.

The coupling between bone resorption and bone formation involves the regulation of a number of soluble factors produced by both osteoclasts and osteoblasts that can be either paracrine (produced by

one cell type to influence the other cell type) or autocrine (produced by one cell type to influence its own cell type), as illustrated in Figure 1 [5, 11]. The number of factors involved in this process is enormous and so, for the purpose of this work, only the most relevant ones will be mentioned and considered.

Osteoblasts paracrine factors are factors produced by osteoblasts that influence osteoclasts, and include factors like the receptor activator of nuclear factor κ B ligand (RANKL) and osteoprotegerin (OPG), which bind to the receptor activator of nuclear factor κ B (RANK), present in the surface of osteoclast precursor cells [11]. When RANKL binds to RANK it stimulates the differentiation and activation of osteoclasts. OPG, on the other side, is a soluble decoy receptor that binds to RANKL preventing its binding with RANK, leading to a negative regulation of RANKL activity. The RANKL/OPG ratio determines the degree of osteoclast differentiation and function [12, 10].

Examples of factors produced by osteoblasts that have an influence in osteoblasts (osteoblasts autocrine factors) are the insulin-like growth factor (IGF), responsible for recruiting osteoblasts to sites of bone resorption and *Wnt*, which is indispensable for osteoblast differentiation and activation. *Wnt* co-receptors activate β -catenin, leading to an upregulation of transcription factors that are crucial for osteoblast differentiation. In differentiated osteoblasts, *Wnt*-signaling also plays an important role in stimulating OPG and inhibiting RANKL, thereby negatively regulating osteoclast formation [5, 11].

The transforming growth factor (TGF)- β is the predominant factor produced by osteoclasts and is an example of both osteoclast paracrine and autocrine regulation. Bone matrix is the largest source of TGF- β in the body. It is released by osteoclasts during the process of bone resorption, and is capable of stimulating the recruitment of osteoblasts and the migration and proliferation of osteoblast precursors. At the same time, TGF- β induces osteoclast apoptosis [12, 11].

2.2. Mechanical Stimulus

Bone tissue is able to adapt to changes in its mechanical environment. [5, 15]. Osteocytes are considered to be the major cell type responsible for sensing mechanical strain and respond with signals of resorption and formation (Figure 1) [16]. When mechanically stimulated, osteocytes expression of OPG increases, decreasing the RANKL/OPG ratio and, consequently, down-regulating osteoclastogenesis. Furthermore, mechanically challenged osteocytes release nitric oxide (NO), which is a strong inhibitor of bone resorption that suppresses the expression of RANKL and increases the expression of OPG, and TGF- β , also contributing to the decrease in osteoclastogenesis. Osteocytes also play a role in stimulating osteoblasts formation and activation by inducing β -catenin signaling, which leads to the expression of *Wnt* targets [15, 5, 8, 18, 3, 16].

Osteoblasts are the second major type of cell to sense and respond to mechanical stimulus, though its response is very similar to the one from osteocytes. When exposed to strain, osteoblasts reduce the expression of RANKL, decreasing osteoclast number. Like osteocytes, osteoblasts also release NO, responsible for decreasing the RANKL/OPG ratio, downregulating osteoclast formation and activation. In addition, osteoblasts subjected to mechanical strains increase the production of *Wnt*, upregulating its own differentiation and activation [15, 8, 18, 16, 9]. Mechanical stimulus also affects osteoclasts but, although these effects are not yet well understood, they seem to be indirect, adding another layer of control by which mechanical force might limit bone resorption [15, 16].

2.3. Myeloma Bone Disease

Multiple myeloma (MM) is a hematological malignancy, known to induce increased osteoclastic bone resorption, while osteoblast activity is severely decreased or absent, uncoupling the process of bone remodeling in areas adjacent to myeloma cells: there are large numbers of osteoclasts with no reactive new bone formation and no osteoblastic response(Figure 1) [4, 2]. In addition, interactions between myeloma cells and cells of the bone marrow microenvironment induce myeloma growth and survival (Figure 1), and stimulate the development of osteolytic lesions [2].

In MM, osteoclast activity is increased due to the release of osteoclastogenic factors, produced by MM cells, which act decreasing the production of OPG and stimulating the production of RANKL, leading to an increase in the RANKL/OPG ratio [4]. MM cells also promote the production of two other factors that play a role in osteoclastogenesis: macrophage inflammatory protein-1 α (MIP-1 α), a chemokine produced by MM cell to stimulates the production of RANKL and IL-3, which enhances the effects of RANKL and MIP-1 α [4]. In addition, IL-3 and other growth factors [6] released during the bone destructive process are able to stimulate MM cell growth, creating what Abe *et al.* [1] describes as a "vicious cycle", in which the growth factor released during the bone resorptive process increase MM tumor burden, which in turn increases bone destruction [4, 1].

Despite there is significantly less information related to the influence of MM cells on osteoblasts, it

is known that they decrease the activity of Wnt by producing a Wnt antagonist, which downregulates osteoblast differentiation and activation [13]. Other studies [4, 6] also suggest that the production of $TGF-\beta$, an inhibitor of osteoblast differentiation, is increased in MM patients. It is interesting to notice that the influence of the myeloma cells on the interactions between bone cells is opposite to the one triggered by the mechanical stimulus (Figure 1).

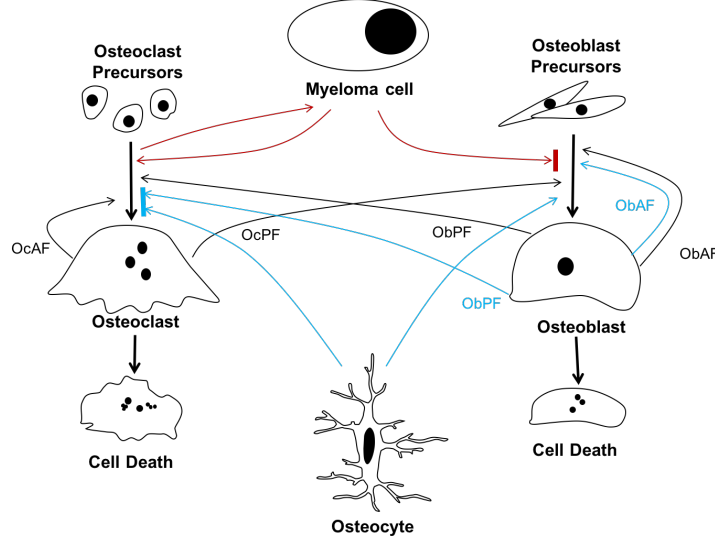


Figure 1: Schematic representation of the interactions between bone cells: osteoclasts autocrine factors (OcAF), osteoclasts paracrine factors (OcPF), osteoblasts autocrine factors (ObAF) and osteoblasts paracrine factors (ObPF). The black arrows represent the interactions between cells under normal circumstances, the blue arrows represent the effects of the mechanical stimulus on those interactions, and the red arrows represent the effects of the myeloma bone disease.

3. Model Development

To replicate the biochemical processes involved in bone remodeling, as well as the corresponding bone mechanical environment, a set of differential equations were created, and solved using a numerical integration algorithm in Matlab. A finite element model was then created using ABAQUS in order to include the mechanical stimulus and observe the density distribution in the bone.

According to the model described by Komarova *et al.* [11], and later reviewed by Ayati *et al.* [2], the dynamics of cell populations at the bone remodeling site is described by the following system of differential equations

$$\frac{dC(t)}{dt} = \alpha_C C(t)^{g_{CC}} B(t)^{g_{BC}} - \beta_C C(t) \quad (1a)$$

$$\frac{dB(t)}{dt} = \alpha_B C(t)^{g_{CB}} B(t)^{g_{BB}} - \beta_B B(t) \quad (1b)$$

where $C(t)$ and $B(t)$ are, respectively, the number of osteoclasts and osteoblasts; α_i is the activity of cell production (α_C - production of osteoclasts, α_B - production of osteoblasts) and β_i is the activity of cell removal (β_C - removal of osteoclasts, β_B - removal of osteoblasts). The parameters g_{ij} represent the net effectiveness of osteoclast- or osteoblast-derived autocrine or paracrine factors (g_{CC} - osteoclast-derived autocrine factor, g_{CB} - osteoclast-derived paracrine factor, g_{BB} - osteoblast-derived autocrine factor, g_{BC} - osteoblast-derived paracrine factor), which reflect the amount of effector produced per donor cell as well as the responsiveness of the target cell.

The model includes a third equation describing the changes in bone mass. To build this equation it was assumed that the number of active cells is a percentage of the total number of cells and, this way, the bone mass is affected by both increases and decreases in the number of activated cells. The bone mass equation is as follows

$$\frac{dz(t)}{dt} = (-k_C C(t) + k_B B(t))S(z(t)) \quad (2)$$

where

$$S(z(t)) = z(t)(1.73 - z(t)) \quad (3)$$

In this equation, $z(t)$ is the total bone mass and k_i is the normalized activity of bone (K_C - bone resorption, K_B - bone formation). In addition, the equation was multiplied by a surface function, $S(z(t))$, because cellular actions begin at the surface of the bone, so its potential is directly dependent on the amount of surface. This function equals zero when the bone density is zero or when it assumes its maximum value ($S(0) = 0$ and $S(1.73) = 0$), and reaches a maximum value when the density equals half its maximum.

The mechanical loading, in this case considered as strain energy [7], influences the net effectiveness parameters (g_{ij} in equations 1) and, for this reason, a term dependent on the strain energy density (SED) was added to these parameters. In addition, considering that osteocytes are the cells primarily responsible for sensing the mechanical stimulus, producing a response that can affect both osteoclasts and osteoblasts, a term related to the influence of the osteocytes response to the mechanical stimulus was added to equations 1. The biomechanicochemical model is then given by

$$\frac{dC(t)}{dt} = \alpha_C C(t)^{g_{CC} + \xi_{CC} \left(\frac{\Psi(t)}{\bar{\Psi}} - 1\right)} B(t)^{g_{BC} + \xi_{BC} \left(\frac{\Psi(t)}{\bar{\Psi}} - 1\right)} - \beta_C C(t) + O_C \left(\frac{\Psi(t)}{\bar{\Psi}} - 1\right) \quad (4a)$$

$$\frac{dB(t)}{dt} = \alpha_B C(t)^{g_{CB} + \xi_{CB} \left(\frac{\Psi(t)}{\bar{\Psi}} - 1\right)} B(t)^{g_{BB} + \xi_{BB} \left(\frac{\Psi(t)}{\bar{\Psi}} - 1\right)} - \beta_B B(t) + O_B \left(\frac{\Psi(t)}{\bar{\Psi}} - 1\right) \quad (4b)$$

$$\frac{dz(t)}{dt} = (-k_C C(t) + k_B B(t)) S(z) \quad (4c)$$

where ξ_{ij} are constants that represent the weight of the mechanical term to the respective g_{ij} parameter, the constants O_i represent the influence of the osteocytes response, Ψ is the SED at time t and $\bar{\Psi}$ is a threshold value.

The cells affected by myeloma bone disease behave differently than the not affected cells and cannot be described by the same model. Ayati *et al.*[2] modeled the influences of tumor growth on bone remodeling, with a special insight on how the tumor influences autocrine and paracrine signaling in the osteoclast and osteoblast cell populations. Introducing these influences on equations 4, the equations for cancer cells are

$$\frac{dC(t)}{dt} = \alpha_C C(t)^{g_{CC} + g_{CC} r_{CC} \frac{T(t)}{L_T} + \xi_{CC} \left(\frac{\Psi(t)}{\bar{\Psi}} - 1\right)} B(t)^{g_{BC} + g_{BC} r_{BC} \frac{T(t)}{L_T} + \xi_{BC} \left(\frac{\Psi(t)}{\bar{\Psi}} - 1\right)} - \beta_C C(t) + O_C \left(\frac{\Psi(t)}{\bar{\Psi}} - 1\right) \quad (5a)$$

$$\frac{dB(t)}{dt} = \alpha_B C(t)^{g_{CB} + \left[\frac{g_{CB}}{1 + r_{CB} \frac{T(t)}{L_T}} - g_{CB}\right] + \xi_{CB} \left(\frac{\Psi(t)}{\bar{\Psi}} - 1\right)} B(t)^{g_{BB} - r_{BB} \frac{T(t)}{L_T} + \xi_{BB} \left(\frac{\Psi(t)}{\bar{\Psi}} - 1\right)} - \beta_B B(t) + O_B \left(\frac{\Psi(t)}{\bar{\Psi}} - 1\right) \quad (5b)$$

$$\frac{dT(t)}{dt} = \gamma_T T(t) \log \left(\frac{L_T}{T(t)} \right) \quad (5c)$$

$$\frac{dz(t)}{dt} = (-k_C C(t) + k_B B(t)) S(z) \quad (5d)$$

where $C(t)$ and $B(t)$ are, respectively, the number of osteoclasts and osteoblasts, as before, and $T(t)$ is the density of tumor cells at time t . The tumor equation (equation 5c) is of Gompertz form with growth constant γ_T (positive and independent of bone loss) and maximum tumor size L_T . The parameters r_{ij} represent the influence of the tumor on each net effectiveness parameter.

The dynamic behavior of the system of equations 4 and 5 was analyzed using numerical integration by a fourth-order Runge-Kutta algorithm in Matlab, which is an iterative method used to obtain the approximate solutions of ODEs. A finite element model (FEM) of a 2D femur bone (Figure 2), with 2403 linear tetrahedral elements (1292 nodes), was created using ABAQUS in order to obtain the mechanical stimulus, the strain energy value, in each node.

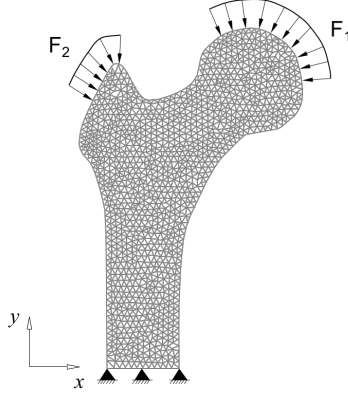


Figure 2: Computational model for a 2D femur bone. The model has 2403 tetrahedral elements (1292 nodes), and is fixed at the bottom. The forces were applied on the femur's head ($F_{1x} = -224N$, $F_{1y} = -2246N$) and trochanter ($F_{2x} = 768N$, $F_{2y} = 1210N$).

The routine implemented in Matlab computes the number of bone cells (osteoclasts and osteoblasts), as well as the bone mass for each node of the model, meaning that the number of equations to be solved is determined by the number of elements of the model. In this mathematical model, bone is considered an isotropic material, with two material properties: Poisson's coefficient ($\nu = 0.3$) and Young's modulus, determined according to the following power law

$$E = 3790z^3 \quad (6)$$

where $E[MPa]$ is the Young's Modulus and the density, z , varies between 0 and $1.73gcm^{-3}$.

4. Results

The results for the biochemical model (equations 1 and 2) are presented in Figure 3. The initial values and parameters for these equations are presented in Table 1, and are according to [11].

$t_{initial}$	0 days
t_{final}	150 days
$C(0)$	11.06 cells
$B(0)$	212.13 cells
$z(0)$	$0.865 gcm^{-3}$
\bar{C}	1.06 cells
\bar{B}	212.13 cells
α_C	3 cells day^{-1}
α_B	4 cells day^{-1}
β_C	0.2 day^{-1}
β_B	0.02 day^{-1}
g_{CC}	0.5
g_{CB}	1.0
g_{BC}	-0.5
g_{BB}	0.0
k_C	$0.0037 gcm^{-3} \text{ cell}^{-1} \text{ days}^{-1}$
k_B	$0.0000185 gcm^{-3} \text{ cell}^{-1} \text{ day}^{-1}$

Table 1: Initial values and parameters of the model.

In this case, the bone remodeling process was triggered by an initial increase in the number of osteoclasts, with respect to the steady-state condition. It is possible to see that both the number of cells and the bone mass are the same for each node of the model, as Figures 3(a), 3(b) and 3(c) present only one line, which is, in fact, an overlap of the 1292 lines (one for each node of the model). In addition, Figure 3(d) shows that the bone mass distribution is homogeneous along the femur model. It is also

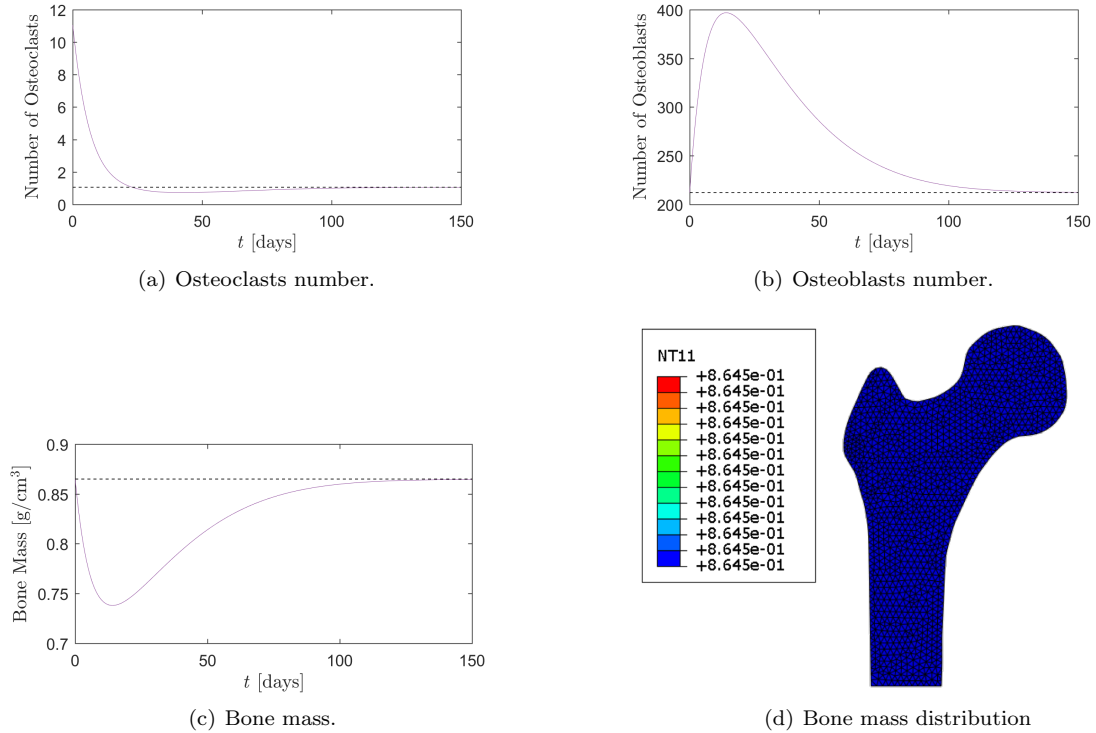


Figure 3: Results obtained with the biochemical model (equations 1) and the bone mass equation (equation 2)

possible to see that, after the initial perturbation in the number of osteoclasts, the solution converges for the steady-state conditions after 150 days. The results show that the initial increase in the number of osteoclasts leads to a decrease in the bone mass, to which the system responds increasing the number of osteoblasts to form new bone and reestablish the equilibrium.

The results after introducing the mechanical stimulus in the biochemical model (equations 4) are presented in Figure 4. In this case, $C(0)$ equals its steady-state value, and the remodeling process is triggered by an external mechanical stimulus. The new parameters of equations 4 were assumed to be as follows: $O_C = -0.01$, $O_B = 2$, $\xi_{BC} = -0.1$, $\xi_{BB} = 0.2$. Due to the low influence of osteoclasts response to mechanical stimulus, the parameters ξ_{CC} and ξ_{CB} were assumed to be zero. The values admitted for these parameters take into account two main aspects: (1) the order of magnitude of the other terms of the equations, as the g_{ij} parameters; (2) its influence on the convergence and stability of the solution. The value $\bar{\Psi}$ was assumed to be an average value of the SED of each node, obtained with the biochemical model.

The first conclusion to withdraw is that the introduction of the mechanical stimulus leads to a solution that is no longer homogeneous, in which each node has a different concentration of osteoclasts and osteoblasts and the bone mass is distributed according to the demands of the mechanical environment. In addition, the results show formation of a medullary channel, with higher values of bone mass in the diaphysis walls and values close to zero between them, and the formation of the Ward's triangle, proving to be a good representation of the biological situation. However, Figure 4(c) shows that the bone mass is not stabilized after 150 days.

To test the influence of the myeloma bone disease, together with the influence of the mechanical stimulus, the tumor case presented in Figure 5 was considered. The values assumed for the parameters of equations 5 are the same as the previous analysis, plus the cancer parameters: $\gamma_T = 0.05$, $L_T = 100$, $r_{BC} = 0$, $r_{CB} = 0$, $r_{BB} = 0.2$ and $r_{CC} = 0.005$, which were set according to what is described by Ayati *et al.* [2]. Figure 6 shows the evolution of the tumor cells after 250 days, and it is possible to see that it reaches 100% of its size a few days after the remodeling cycle begins.

Figure 7 is presented as a reference, since this analysis corresponds to the same analysis presented in Figure 4, but in this case the cells that will suffer the influence of the myeloma are highlighted in order to facilitate a posterior comparison of their behavior with, and without the influence of myeloma, and

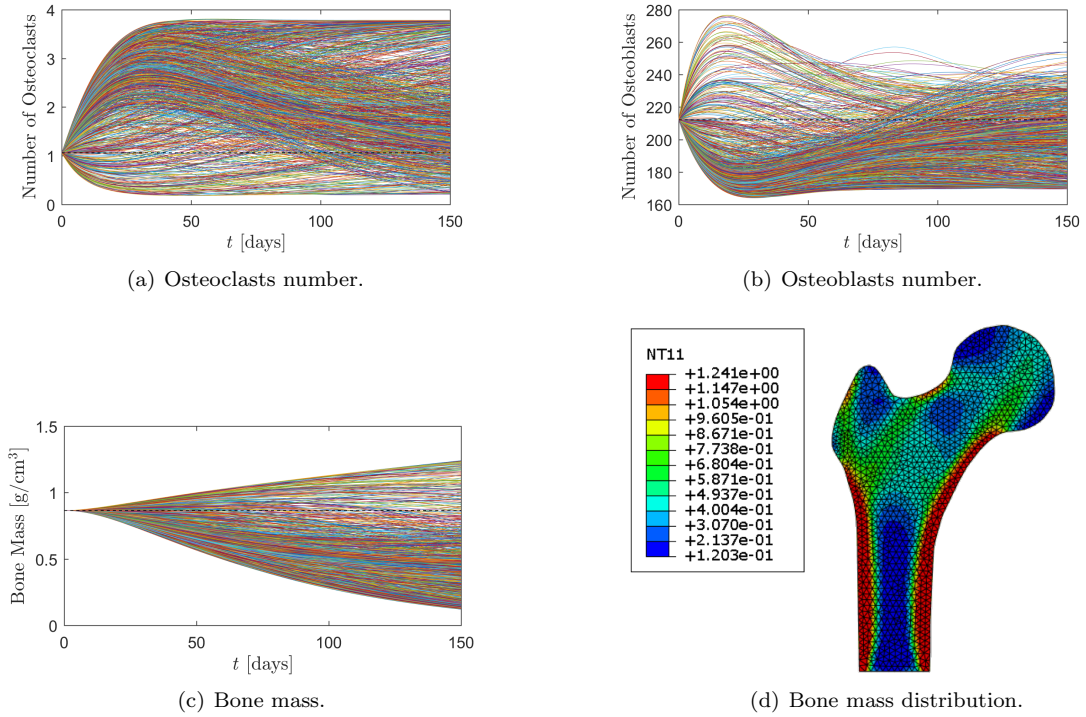


Figure 4: Results for the biomechanochemical model, with $O_C = -0.01$, $O_B = 2$, $\xi_{BC} = -0.1$, $\xi_{BB} = 0.2$



Figure 5: Location of the tumor considered for the analysis of myeloma bone disease.

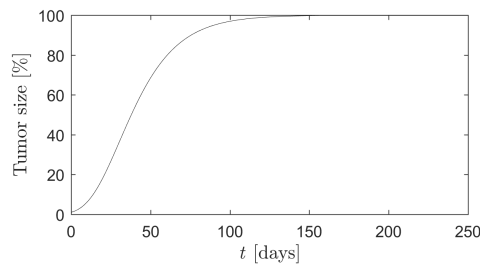


Figure 6: Evolution of the tumor.

withdraw some conclusions about the effects of the disease.

Figures 8 are the results for the system of equations 5. Comparing Figure 8 with Figure 7, it is possible to see that the number of osteoclasts in the nodes affected by the tumor (Figure 8(a)) increased, and the number of osteoblasts suffered a significant decrease (Figure 8(b)). Consequently, the values of bone mass for these nodes are lower in Figure 8(c) when compared to Figure 7(c). These results are according to what was expected, since the myeloma bone disease stimulates the formation and activation of osteoclasts, while inhibiting osteoblast action. Figure 8(d) shows a region of low density (close to zero)

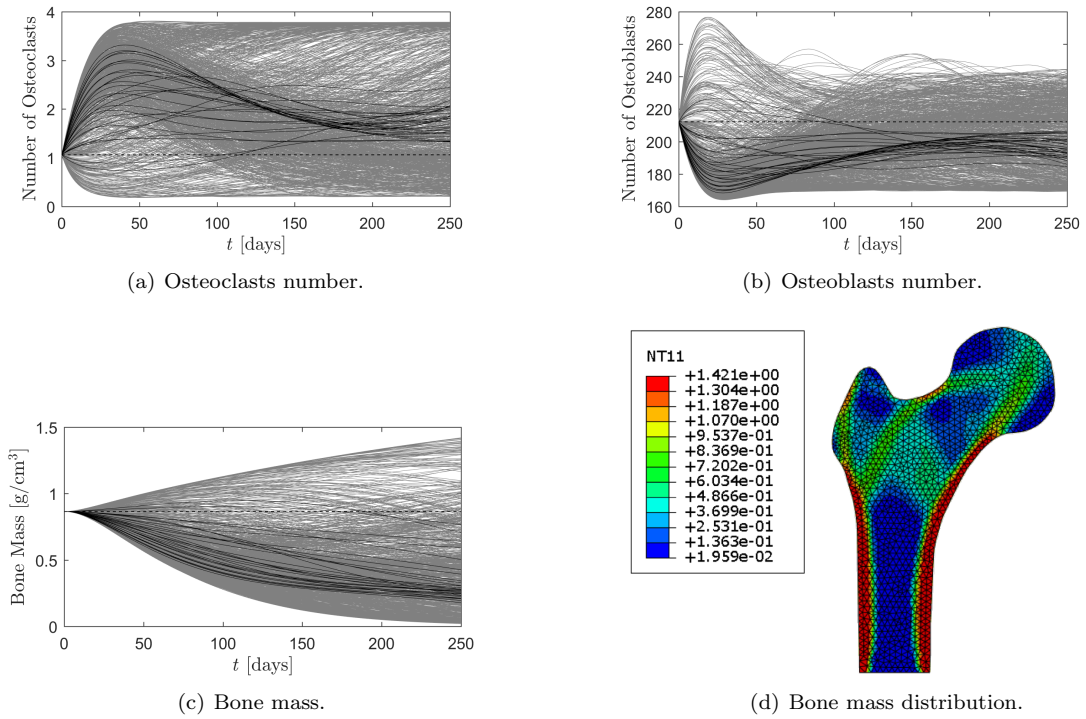


Figure 7: Reference results.

in the place where the tumor was set. This low density region corresponds to what is known as the osteolytic bone disease.

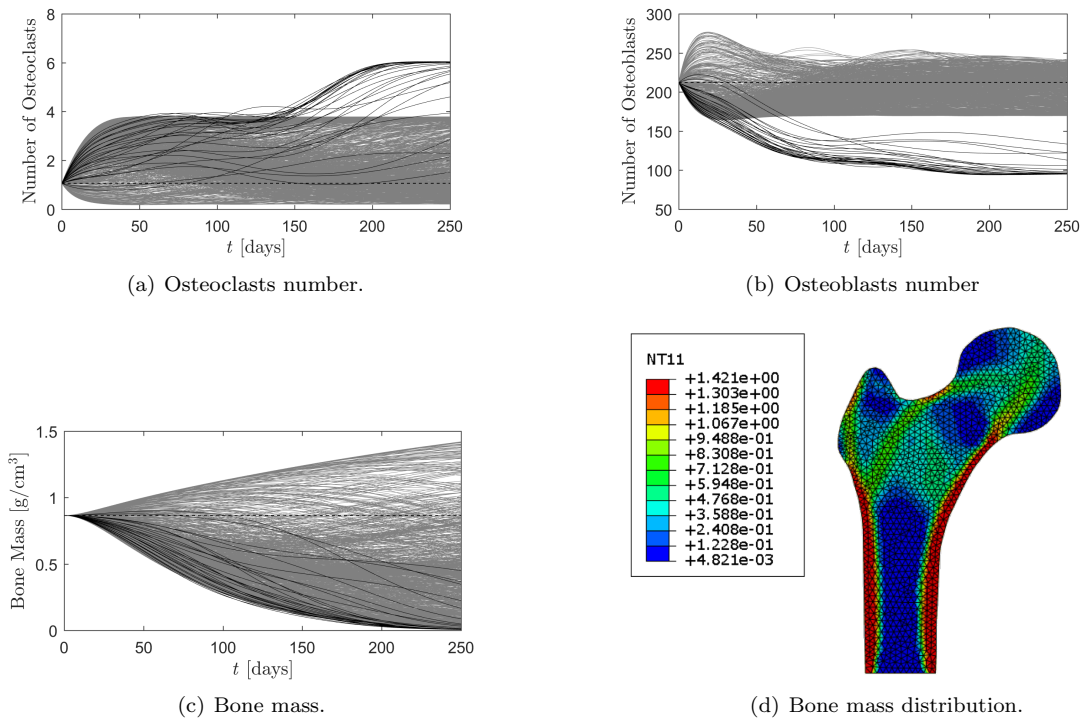


Figure 8: Results for equations 5.

5. Conclusions

The development of models that reproduce the biochemical and biomechanical interactions between bone cells during the process of bone remodeling is important to better understand the behavior of bone under different circumstances, for instance, abnormal load carrying situations or diseases. The biochemical model proved to be a good representation of the biochemical environment of bone and of the activity of bone cells and their interactions. However, since this model does not include the influence of the mechanical stimulus, it fails in addressing the bone mass to places of higher demand, leading to a homogeneous distribution of bone density that does not happen in the biological environment.

The introduction of the mechanical stimulus lead to a solution that was no longer homogeneous, with bone mass being addressed according to the mechanical demand. In these results it was possible to observe that bone was forming a medullary channel, with higher values of bone density in regions correspondent to the diaphysis walls, and values close to zero between them, which is in agreement with the biological situation. In addition, it was possible to observe the formation of Wards triangle on the femurs neck. More tests and biological studies would be important to understand the evolution of the concentration of bone cells, throughout the whole process of bone remodeling, in different sites of the mechanically stimulated bone.

For the case of tumor tested, the myeloma bone disease showed to have the expected influence on the affected nodes: there was an increase in the number of osteoclasts, followed by a substantial decrease in the number of osteoblasts, which consequently lead to a decrease in the bone mass. However, as the theory states that not only the cells of myeloma affect both osteoclasts and osteoblasts, but also osteoclasts have an important influence in the activation and proliferation of myeloma cells, the addition of a term dependent on the number of osteoclasts to the tumor equation should be considered. Moreover, as the myeloma cells seem to have a direct influence on both osteoclasts and osteoblasts, the effects of the addition of a term dependent on the myeloma cells, in the equations of bone cells, should be tested. The model should also be expanded to include the influence of the treatments for myeloma bone disease.

One limitation of this model is that it does not consider the possible phenomena of the migration of bone cells to different sites of bone. As future work, it would also be interesting to adapt the model to include the diffusion of both bone cells and tumor cells. Moreover, it would be interesting to test the equations in different types of bones as, for example, the vertebral bodies or the ribs, as they are sites of red marrow and are the bones most commonly affected by multiple myeloma. Lastly, it would be important to test the influence of multiple loads on the bone.

Acknowledgements

This work was supported by FCT, through IDMEC, under LAETA, project UID/EMS/50022/2013 and project LAETA, BoneSys Bone biochemical and biomechanical integrated modeling: addressing remodeling, disease and therapy dynamics.

References

- [1] M. Abe, K. Hiura, J. Wilde, A. Shioyasono, K. Moriyama, T. Hashimoto, S. Kido, T. Oshima, H. Shibata, S. Ozaki, D. Inoue, and T. Matsumoto. Osteoclasts enhance myeloma cell growth and survival via cell-cell contact: a vicious cycle between bone destruction and myeloma expansion. *Blood*, 104(8):2484–2491, Oct. 2004. doi:10.1182/blood-2003-11-3839.
- [2] B. P. Ayati, C. M. Edwards, G. F. Webb, and J. P. Wikswo. A mathematical model of bone remodeling dynamics for normal bone cell populations and myeloma bone disease. *Biology Direct*, 5:1–17, May 2010. doi:10.1158/0008-5472.CAN-13-2652.
- [3] L. F. Bonewald and M. L. Johnson. Osteocytes, mechanosensing and wnt signaling. *Bone*, 42:606–615, Dec. 2008. doi:10.1016/j.bone.2007.12.224.
- [4] R. Coleman, P.-A. Abrahamson, and P. Hadji. *Handbook of Cancer-Related Bone Disease*. BioScientifica, second edition, jul 2012.
- [5] J. C. Crockett, M. J. Rogers, F. P. Coxon, L. J. Hocking, and M. H. Helfrich. Bone remodelling at a glance. *Journal of Cell Science*, 124(7):991–998, 2011. doi:10.1242/jcs.063032.
- [6] C. M. Edwards, J. Zhuang, and G. R. Mundy. The pathogenesis of the bone disease of multiple myeloma. *Bone*, 42:1007–1013, Jan. 2008. doi:10.1016/j.bone.2008.01.027.

- [7] R. Huiskes, H. Weinans, H. J. Grootenboer, M. Dalstra, B. Fudala, and T. J. Slooff. Adaptive bone-remodeling theory applied to prosthetic-design analysis. *Journal of Biomechanics*, 20(11):1135–1150, Sept. 1987. doi:10.1016/0021-9290(87)90030-3.
- [8] C. R. Jacobs, S. Temiyasathit, and A. B. Castillo. Osteocyte mechanobiology and pericellular mechanics. *Annual Review of Biomedical Engineering*, 12:369–400, Dec. 2010. doi:10.1146/annurev-bioeng-070909-105302.
- [9] D. B. Jones, H. Nolte, J.-G. Scholubbers, E. Turner, and D. Veltel. Biochemical signal transduction of mechanical strain in osteoblast-like cells. *Biomaterials*, 12:101–110, Mar. 1991. doi:0142-9612/91/020101-10.
- [10] S. V. Komarova. Bone remodeling in health and disease: Lessons from mathematical modeling. *Annual New York Academy of Sciences*, 1068:557–559, 2006. doi:10.1196/annals.1346.052.
- [11] S. V. Komarova, R. J. Smith, S. J. Dixon, S. M. Sims, and L. M. Wahl. Mathematical model predicts a critical role for osteoclast autocrine regulation in the control of bone remodeling. *Bone*, 33:206–215, Mar. 2003. doi:10.1016/S8756-3282(03)00157-1.
- [12] V. Lemaire, F. L. Tobin, L. D. Greller, C. R. Cho, and L. J. Suva. Modeling the interactions between osteoblast and osteoclast activities in bone remodeling. *Journal of Theoretical Biology*, 229:293–309, Mar. 2004. doi:10.1016/j.jtbi.2004.03.023.
- [13] T. Oshima, M. Abe, J. Asano, T. Hara, K. Kitazoe, E. Sekimoto, Y. Tanaka, H. Shibata, T. Hashimoto, S. Ozaki, S. Kido, D. Inoue, and T. Matsumoto. Myeloma cells suppress bone formation by secreting a soluble wnt inhibitor, sfrp-2. *Blood*, 106(9):3160–3165, Nov. 2005. doi:10.1182/blood-2004-12-4940.
- [14] P. Pivonka, P. R. Buenzil, S. Scheiner, C. Hellmich, and C. R. Dunstan. The influence of bone surface availability in bone remodeling - a mathematical model including coupled geometrical and biomechanical regulations of bone cells. *Engineering Structures*, 47:134–147, Nov. 2013. doi:10.1016/j.engstruct.2012.09.006.
- [15] A. G. Robling, A. B. Castillo, and C. H. Turner. Biomechanical and molecular regulation of bone remodeling. *Annual Review of Biomedical Engineering*, 8:455–498, Apr. 2006. doi:10.1146/annurev.bioeng.8.061505.095721.
- [16] J. Rubin, C. Rubin, and C. R. Jacobs. Molecular pathways mediating mechanical signaling in bone. *Gene*, 367:1–16, Dec. 2006. doi:10.1016/j.gene.2005.10.028.
- [17] S. Scheiner, P. Pivonka, and C. Hellmich. Coupling systems biology with multiscale mechanics, for computer simulations of bone remodeling. *Computer methods in applied mechanics and engineering*, 254:181–196, Oct. 2013. doi:10.1016/j.cma.2012.10.015.
- [18] L. You, S. Temiyasathit, P. Lee, C. H. Kim, P. Tummala, W. Yao, W. Kingery, A. M. Malone, R. Y. Kwon, and C. R. Jacobs. Osteocytes as mechanosensors in the inhibition of bone resorption due to mechanical loading. *Bone*, 42:172–179, Sept. 2008. doi:10.1016/j.bone.2007.09.047.